Gapped Spectrum Shaping for Tandem-Hopped Radar/Communications & Cognitive Sensing

John Jakabosky[1,2], Brandon Ravenscroft[1], Shannon D. Blunt[1], and Anthony Martone[3]
[1]University of Kansas – Radar Systems Lab, Lawrence, KS, USA
[2]Naval Research Laboratory – Radar Division, Washington, DC, USA
[3]Army Research Laboratory, Adelphi, MD, USA

***Abstract* – A non-repeating FMCW waveform was recently developed and experimentally demonstrated to provide a feasible instantiation of FM noise radar. This emission scheme was subsequently examined in terms of the impact of both stationary and hopped spectral gaps with the prospect of enabling in-band interference avoidance for cognitive sensing and possibly tandem hopped radar/communications. Here this gap-hopped spectrum framework is further explored with regard to the relation between the shaping of spectral gaps and the associated time sidelobe response. Experimental loopback measurements are shown that provide a sense of how this form of emission would operate on a real system.**

I. Introduction

While radar spectrum continues to be heavily contested from a regulatory perspective, ongoing research in spectrum engineering and waveform diversity [1,2] are seeking technical solutions. For example, the ongoing DARPA SSPARC program is investigating how radar and communication systems may cohabitate the same spectrum. Likewise, there is considerable ongoing work on specific aspects of cognitive radar to facilitate the means to sense and avoid other spectrum users (e.g. [3, 4]).

Here we leverage a recent new FM continuous wave (FMCW) waveform [5] that possesses the rather useful property of never repeating, while still maintaining a constant envelope (attractive for high power emission) and being well-contained spectrally (with obvious utility in this context). Denoted as pseudo-random optimized (PRO) FMCW, this waveform has been experimentally demonstrated to achieve low range sidelobes and to be amenable for clutter cancellation to perform moving target detection. It has also been shown [6] that this waveform provides a useful framework within which to incorporate spectral gaps. The reason is that that increase in range sidelobes that usually accompanies the inclusion of spectral gaps is to some degree offset by the fact that the sidelobes do not coherently combine within the changing signal structure. A fundamental difference between this approach and existing gapped spectrum approaches [7-14], is that this waveform does not repeat. In this paper the spectrally gapped PRO-FMCW waveform is examined with regards to shaping of the gaps to further reduce range sidelobes and this approach is experimentally measured to evaluate feasible gap depth in the presence of transmitter distortion. The specific applications envisioned for this manner of waveform are cognitive avoidance of in-band interferers and tandem-hopped radar and communications, where the latter involves embedding an information-bearing signal within the gaps that is akin to frequency-hopped spread spectrum [15,16].

II. Spectrally Shaped Optimization

The PRO-FMCW waveform [5] is produced from pseudo-random initializations and is spectrally shaped on a "segment-wise" basis to produce a favorable autocorrelation response. However, the direct approach realizes spectral gaps that are rectangular in shape and thus produce range sidelobes with a $\sin(x)/x$ shape. In an effort to mitigate these sidelobes, tapering of such spectral gaps is investigated.

First a desired power spectral density (PSD), denoted as $|G(f)|^2$, is selected that will produce low autocorrelation sidelobes. The PSD used here is Gaussian because it likewise produces a Gaussian autocorrelation that ideally exhibits zero range sidelobes. In practice, of course, numerical imprecision and spectral roll-off issues prevent the optimized waveform from matching a Gaussian PSD exactly. However, in [5] range sidelobes below −70 dB were still achieved.

In [6] the PSD was modified as

$$|G(f)| = 0 \quad \text{for} \quad f \in \Omega, \tag{1}$$

where Ω comprises the set of frequency intervals for which spectral gaps are desired. The enforcement of (1) implicitly produces a rectangular shape at the gap edges that corresponds to the $\sin(x)/x$ roll-off of range sidelobes.

Now consider the incorporation of a given spectral gap as

$$|G(f)| = \begin{cases} h_{\mathrm{L}}(f) & \text{for} \quad f \in \Omega_{\mathrm{L}} \\ 0 & \text{for} \quad f \in \Omega \\ h_{\mathrm{U}}(f) & \text{for} \quad f \in \Omega_{\mathrm{U}} \end{cases}, \tag{2}$$

where Ω_{L}, Ω, and Ω_{U} correspond to the frequency intervals of the lower frequency taper, the gap, and the upper frequency taper, respectively. The frequency tapers $h_{\mathrm{L}}(f)$ and $h_{\mathrm{U}}(f)$ are scaled so that they are continuous with the surrounding PSD. In the next section we examine the impact of different tapers.

The overall PRO-FMCW waveform is produced from a set of M unique, optimized segments. The mth segment is initialized with the random phase signal $p_{0,m}(t)$ followed by the alternating application of

$$r_{k+1,m}(t) = \mathbb{F}^{-1}\left\{ |G(f)| \exp\left(j \angle \mathbb{F}\left\{ p_{k,m}(t) \right\} \right) \right\} \tag{3}$$

and

$$p_{k+1,m}(t) = u(t) \exp\left(j \angle r_{k+1,m}(t) \right), \tag{4}$$

where $u(t)$ is a rectangular window of length T, $\angle(\bullet)$ extracts the phase of the argument, $\mathbb{F}$ is the Fourier transform, and

This work was supported in part by ARO under Grant # W911Nf-15-2-0063 and by a subcontract with Matrix Research, Inc. for research sponsored by AFRL under Prime Contract # FA8650-14-D-1722.

978-1-5090-0863-6/16/$31.00 ©2016 IEEE

$\mathbb{F}^{-1}$ is the inverse Fourier transform. After K iterations of (3) and (4), the optimized segment $p_{K,m}(t)$ is obtained.

This process can produce spectral gaps with depths around –20 dB relative to the peak. Deeper gaps are required to mitigate interference and facilitate the embedding of hopped communication signals. The reiterative uniform weight optimization (RUWO) method of [17] was thus used to realize deeper nulls. The mth optimized segment $p_{K,m}(t)$ is discretized into an N-length vector $\mathbf{x}_{0,m}$ that fully encompasses the temporal extent T and is sufficiently "oversampled" with respect to 3 dB bandwidth to capture adequately the spectral roll-off of the segment.

The frequency intervals to null in Ω are discretized into Q values denoted f_q, with Q chosen to achieve sufficient density over the frequencies of interest. An $N \times Q$ matrix of frequency steering vectors is formed using the Q discrete frequencies f_q as

$$\mathbf{B} = \begin{bmatrix} 1 & 1 & \cdots & 1 \\ e^{j2\pi f_0} & e^{j2\pi f_1} & \cdots & e^{j2\pi f_{Q-1}} \\ \vdots & \vdots & & \vdots \\ e^{j2\pi f_0(N-1)} & e^{j2\pi f_1(N-1)} & \cdots & e^{j2\pi f_{Q-1}(N-1)} \end{bmatrix}. \quad (5)$$

Subsequently, the $N \times N$ structured matrix

$$\mathbf{W} = \mathbf{B}\mathbf{B}^H + \delta\mathbf{I} \quad (6)$$

is formed, in which δ is a diagonal loading term and $\mathbf{I}$ is an $N \times N$ identity matrix. Improved gap depth is thus obtained by iteratively applying

$$\mathbf{x}_{l,m} = \exp\left(j\angle\left(\mathbf{W}^{-1}\mathbf{x}_{l-1,m}\right)\right) \quad (7)$$

L times, where the result $\mathbf{x}_{L,m}$, because it was adequately "oversampled" with respect to 3 dB bandwidth initially, closely approximates the continuous signal $x_{L,m}(t)$ that would be obtained from implementation on an arbitrary waveform generator (AWG). Finally, to remove phase discontinuities the mth optimized segment is phase rotated to match that at the end of the $(m-1)$th segment $\phi_{\text{end},m-1}$ via

$$s_m(t) = \exp\left(j\phi_{\text{end},m-1}\right)x_{L,m}(t), \quad (8)$$

where $s_m(t)$ is the mth segment of the gapped waveform.

Receive processing for this non-repeating FMCW is discussed in [5]. Pulse compression can be performed on a per-segment basis followed by Doppler processing across the segments, with the latter serving to suppress sidelobes since they do not coherently combine. Clutter cancellation can also readily be performed. Note that this spectral gapped framework is also applicable to the non-repeating pulsed waveforms developed in [18] using the same spectral shaping design approach.

III. Measured Results

Consider the requirements of achieving both deep spectral gaps and low range sidelobes. Performance of the proposed approach is demonstrated using two different test cases. The first case has a stationary gap for different types of gap tapers. The second case examines the impact of a gap that hops randomly around the band. To evaluate the capability of this approach, a loopback measurement of the waveform in each case was captured. Each waveform was upsampled to 8 GS/s and shifted to a center frequency of 3.55 GHz. The waveform was generated using a Tektronix AWG70K arbitrary waveform generator and subsequently driven 6 dB into saturation on a solid-state amplifier. This compressed waveform was then I/Q-sampled by a Rhode & Schwarz FSW real-time spectrum analyzer at a rate of 200 MS/s. The real-time spectrum analyzer had a capture bandwidth of 160 MHz which produced a noticeable roll-off in spectral power at the edge of the captured spectrum. For both cases, the PRO-FMCW waveform has a length of T_w = 200 ms and is composed of $M = 10^4$ segments. Each segment has an initial 3 dB bandwidth of B = 80 MHz and a length of T = 20 µs. The 3 dB bandwidth of the desired PSD prior to incorporation of a gap is 55 MHz. Thus, each segment of the optimized emission has an approximate time-bandwidth product of 1100.

In addition to the gap from (1), which produces an implicit rectangular taper, we also consider the incorporation of two versions of a Tukey taper in log-scale. Specifically, the first and last half of the rise and fall, respectively, of the log-scale Tukey taper were used so as not to limit the gap depth. The taper on each side of the gap is offset to match the magnitude of the desired PSD, and scaled to a depth of at least –40 dB to match the desired PSD at the boundaries of Ω_L and Ω_U, and to allow for the maximum achievable gap depth. These tapers are in no way claimed to be optimal but are simply used to illustrate the impact that such a tapering effect can have.

In the first case, a single gap of width $B/5$ was placed at the edge of the waveform bandwidth. The taper transitions were allowed to occupy a spectral width of $B/32$ and $B/16$. A waveform with a rectangular gap and a waveform without a gap are also included for reference. The mean PSD of each waveform (after loopback capture) is shown in Figs. 1 and 2. It is observed that the inclusion of a gap slightly increases the out-of-band spectral content, which is to be expected since the waveform remains constant amplitude and the total power output is unchanged. The depth of the gap with or without a taper is approximately –45 dB. This depth is significantly higher than the ideal –70 dB level found in simulation (Fig. 3).

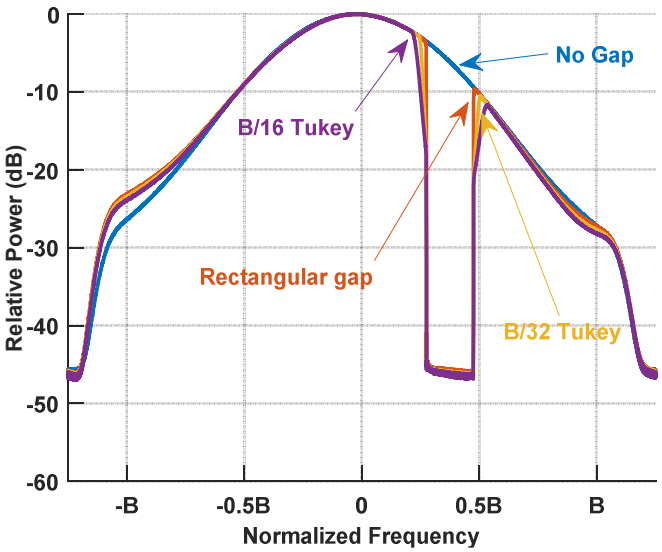

Fig. 1. Mean PSD with a static gap
(loopback measurement with saturated HPA)

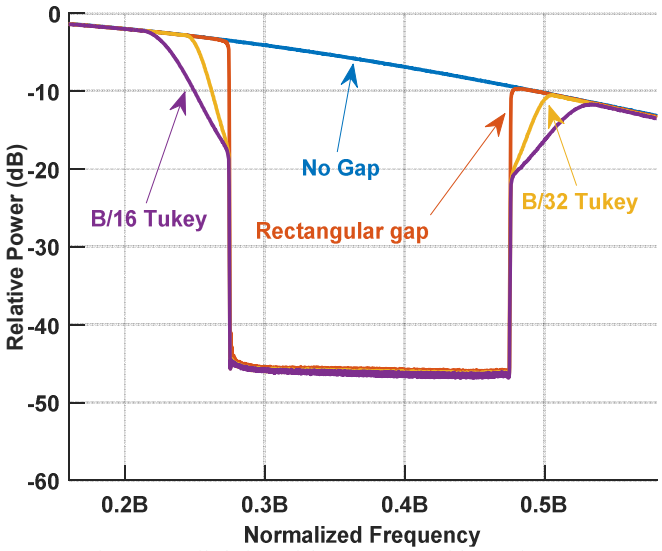

Fig. 2. Detailed view of the mean PSD with a static gap (loopback measurement with saturated HPA)

A comparison of the gap depth using a $B/16$ taper for *a*) the undistorted ideal waveform, *b*) the measured waveform after amplification with a linear amplifier, and *c*) the measured waveform driven into saturation, are shown in Fig. 3. The linear amplifier version is capable of a gap depth of –50 dB while the use of an amplifier driven 6 dB into saturation produced more than 5 dB in degradation to the gap depth. One unexpected result, however, was that very little difference was evident between the simulated and measured autocorrelations. It was also found (not shown) that the measured gap depth is influenced by aliasing resulting from inadequate anti-aliasing filtering within the spectrum analyzer. A higher design sampling rate or narrower waveform bandwidth will enable a greater gap depth.

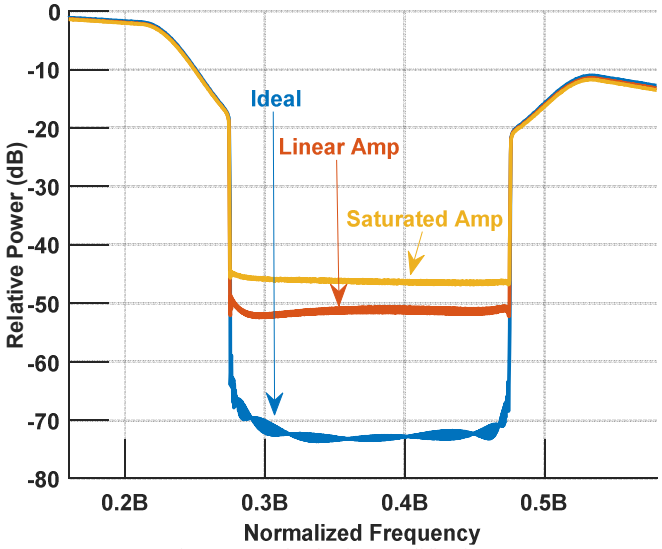

Fig. 3. Gap depth after amplification (idealized, linear amp, and saturated amp)

Now consider the autocorrelation of each segment, followed by coherent integration over the M segments, as depicted by Figs. 4 and 5. The original PRO-FMCW waveform from [5] (the 'no gap' case) realizes sidelobes better than –76 dB. In contrast, the rectangular gap from [6] produces a sidelobe roll-off that extends just beyond $\pm 0.5T$. Using the tapered spectral gaps clearly provides a significant benefit in terms of sidelobe suppression (better than –75 dB), with the $B/32$ Tukey taper achieving roll-off into the sidelobe floor by $0.04T$ and the $B/16$ Tukey taper reaching roll-off into the sidelobe floor by $0.03T$. As one may expect, a widening of the taper width produces a corresponding reduction in the width of the autocorrelation roll-off. For future evaluation, a measure of the quality of the range-sidelobes will need to be incorporated when deciding the appropriate taper width. Some prediction of the autocorrelation sidelobe properties may be possible using methods such as that proposed in [19].

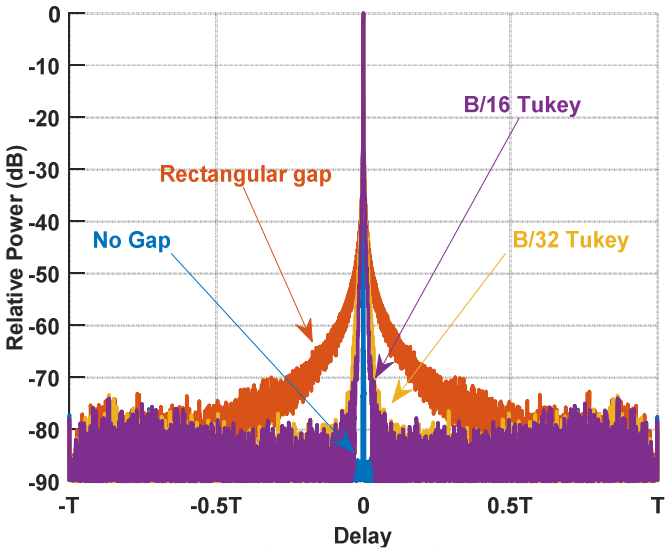

Fig. 4. Integrated autocorrelation with a static gap (loopback measurement with saturated HPA)

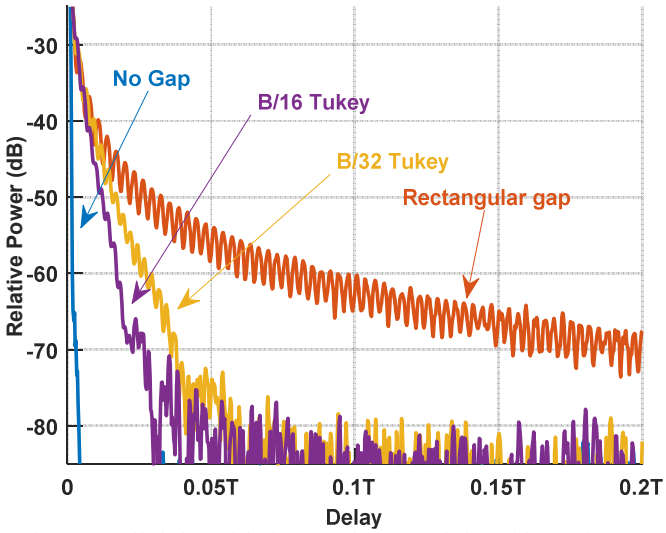

Fig. 5. Detailed view of the integrated autocorrelation with a static gap (loopback measurement with saturated HPA)

In the second case, a spectral gap was randomly hopped within the bandwidth of the waveform to exemplify how a tandem-hopped communication signal might be embedded into the radar emission, if given sufficient gap depth. For the purpose of demonstration, the 10 different gap locations shown in Fig. 6 were used, each with a width of $B/10$. Each gap location was used only once, and the order of use was selected randomly. The $M = 10^4$ segments were divided into 10 subsets of 10^3 contiguous segments, with each subset corresponding to a randomly assigned gap. A $B/32$ Tukey taper was used to reduce the autocorrelation sidelobes. The mean PSD for each subset of segments is shown in Fig. 6, where it is observed that the depth of the gap is strongly related to the relative local power of the spectral envelope. The depth of the gaps is at least −44 dB throughout, while the gaps towards the edge of the band are nearly 3 dB deeper.

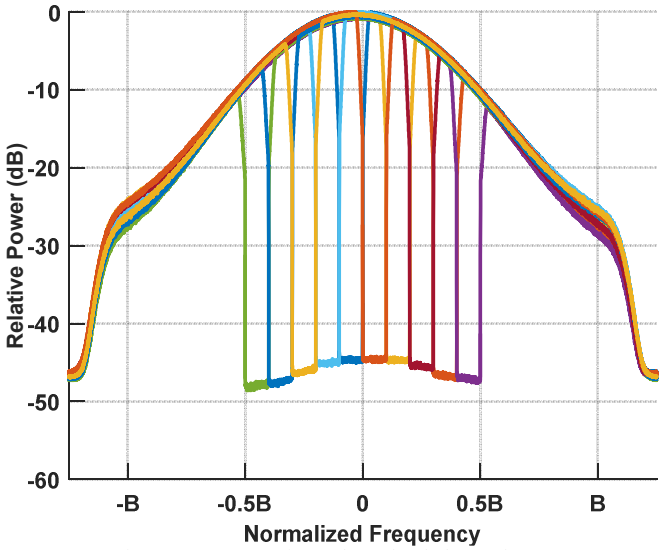

Fig. 6. Mean PSD for each randomly hopped gap (loopback measurement with saturated HPA)

An additional by-product of using hopped gaps with fixed positions and tapering is the distortion of the mean PSD illustrated in Fig. 7. A greater degree of gap overlap would largely eliminate the observed ripple in the mean PSD, which would in turn produce a more favorable autocorrelation. It may also be possible to smooth out this ripple if a much higher number of random overlapping hops were used. An additional effect is a 2 dB increase in the out-of-band spectral roll-off for the randomly hopped waveform as compared to the non-gapped waveform. This result is again expected as the energy displaced from the spectral gaps is conserved.

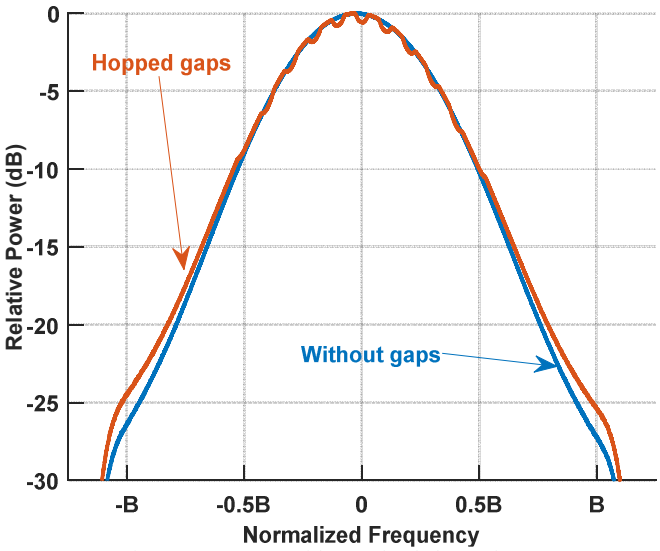

Fig. 7. Mean PSD with a randomly hopped gap (loopback measurement with saturated HPA)

The integrated autocorrelation of randomly hopped gaps is shown in Figs. 8 and 9. The integrated autocorrelation of all hopped gap segments produces an overall autocorrelation with a set of high close-in sidelobes around the mainlobe. The peak sidelobe power is just below −30 dB, though the sidelobes quickly decay to the sidelobe floor by $0.06T$. The structure of these sidelobes is related to the spacing of the gaps placed in the spectrum. Therefore, these sidelobes could potentially be suppressed by using a different set of gap locations. Unsurprisingly, the envelope of the range sidelobes is similar to the envelope of the stationary gap case when using an equivalent taper width of $B/32$.

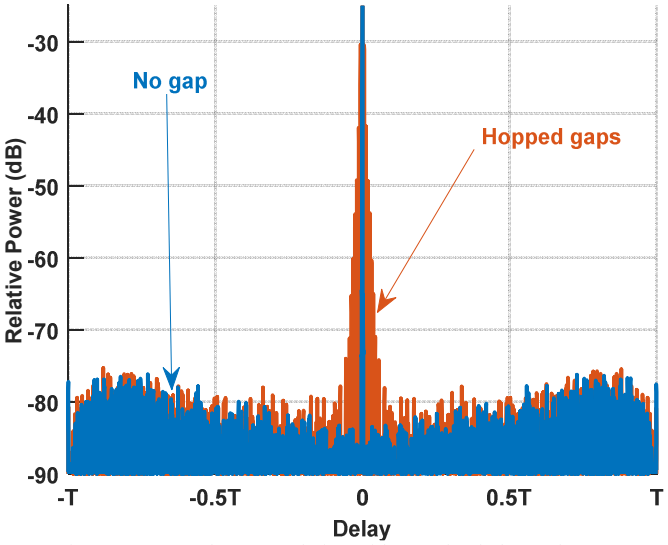

Fig. 8. Integrated autocorrelation with a randomly hopped gap (loopback measurement with saturated HPA)

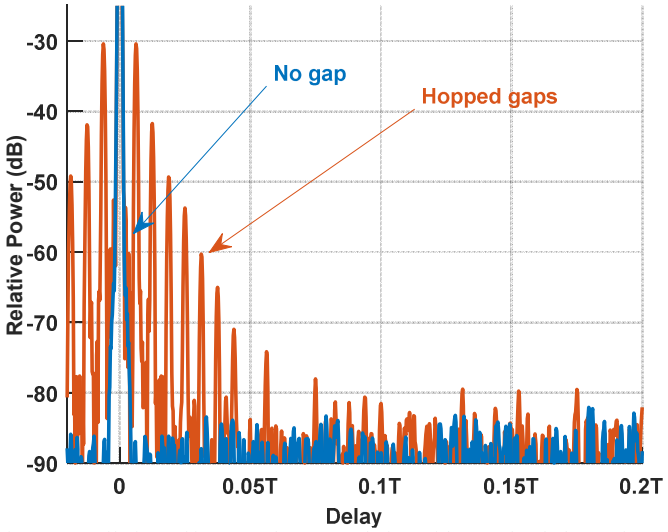

Fig. 9. Detail view of integrated autocorrelation with a randomly hopped gap (loopback measurement with saturated HPA)

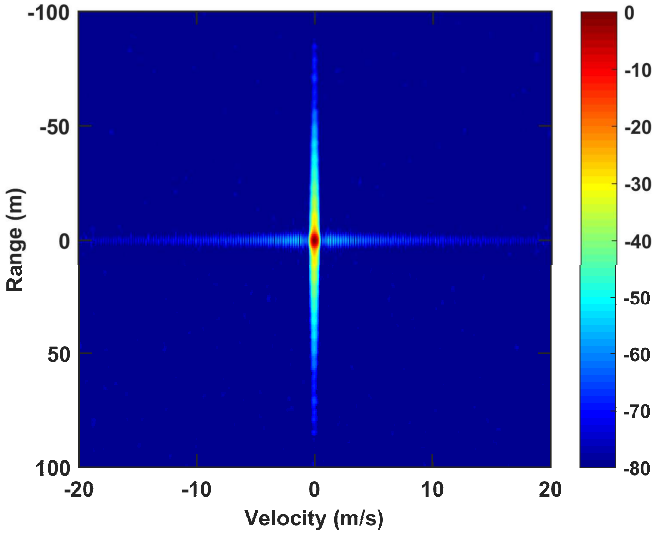

Fig. 10. Range-Doppler point spread function with a static gap

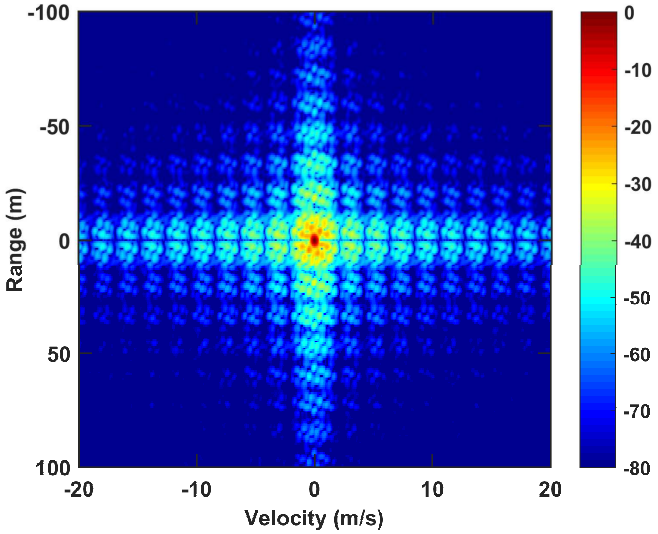

Fig. 11. Range-Doppler point spread function with a randomly hopping gap

The autocorrelation shown in Fig. 8 and 9 assumes a stationary point target. However, the hopping of the spectral gap during the coherent processing interval is expected to produce some degradation when Doppler processing is performed. Each gap location will produce a different range sidelobe shape that is shared by any segment with that same gap location. Likewise, the range sidelobes will change as the gap location changes. This modulation of the range sidelobes will have the effect of producing range and Doppler sidelobes that cannot be easily removed.

To demonstrate this effect, the segments of the *B*/16 Tukey tapered waveform, and the segments of the randomly hopped waveform were pulse-compressed and Doppler processed. Doppler processing was performed by weighting the segments using a Taylor window, and then performing a Fourier-transform across each segment in the 200 ms waveform. These results assume a center-frequency of 3.55 GHz and a pre-optimization bandwidth of 80 MHz.

A zoomed-in region from the range-Doppler point spread function of the *B*/16 Tukey tapered waveform and the randomly hopped waveform are shown in Figs. 10 and 11, respectively. While the zero-Doppler range sidelobes of the *B*/16 waveform are still visible, the Doppler sidelobes of the mainlobe are well suppressed by the Taylor window. However, the randomly hopped waveform has significant energy spread in range and Doppler that was not suppressed by the use of the Taylor window. A radar scene with strong clutter and moving targets would have many of the moving targets obscured by Doppler sidelobes from clutter. Remediation of these range-Doppler sidelobes is a topic of ongoing investigation. It may also be possible to mitigate the Doppler sidelobes to some degree through informed selection of the hopping sequence, the number of hops, and/or the size of the gap.

IV. CONCLUSIONS

Prior work in the design of nonrecurrent nonlinear FMCW waveforms with static and hopping spectral gaps was expanded to include tapering. A significant improvement in the range sidelobe roll-off was produced by rounding the spectral gaps with a taper. The waveform performance was evaluated while under heavy compression from a saturated amplifier. A gap depth of approximately –45 dB was achieved for both the static and hopped waveforms. The impact on Doppler-sidelobes for hopping gaps during the CPI was found to be significant. Ongoing work includes the investigation of methods to mitigate the increased Doppler sidelobes produced by hopping gaps and the evaluation of free-space measurements requiring clutter cancellation.

REFERENCES

[1] H. Griffiths, L. Cohen, S. Watts, E. Mokole, C. Baker, M. Wicks, S. Blunt, "Radar spectrum engineering and management: technical and regulatory issues," *Proc. IEEE*, vol. 103, no. 1, pp. 85-102, Jan. 2015.

[2] H. Griffiths, S. Blunt, L. Cohen, L. Savy, "Challenge problems in spectrum engineering and waveform diversity," *IEEE Radar Conference*, Ottawa, Canada, Apr. - May, 2013.

[3] A.F. Martone, "Cognitive radar demystified," *URSI Bulletin*, no. 350, pp. 10-22, Sept. 2014.

[4] A. Martone, K. Sherbondy, K. Ranney, T. Dogaru, "Passive sensing for adaptive radar bandwidth" *IEEE Intl. Radar Conf.*, Washington, DC, May 2015.

[5] J. Jakabosky, S.D. Blunt, B. Himed, "Waveform design and receive processing for nonrecurrent nonlinear FMCW radar" *IEEE Intl. Radar Conf.*, Washington, DC, May 2015.

[6] J. Jakabosky, S.D. Blunt, A. Martone, "Incorporating hopped spectral gaps into nonrecurrent nonlinear FMCW radar emission," *IEEE Intl. Workshop on Computational Advances in Multi-Sensor Adaptive Processing*, Cancun, Mexico, Dec. 2015.

[7] M.J. Lindenfeld, "Sparse frequency transmit-and-receive waveform design," *IEEE Trans. Aerospace & Electronic Systems,* vol. 40, no. 3, pp. 851-861, July 2004.

[8] M.R. Cook, T. Higgins, A.K. Shackelford, "Thinned spectrum radar waveforms," *Intl. Waveform Diversity & Design Conf.*, Niagara Falls, ON, Canada, Aug. 2010.

[9] K. Gerlach, M.R. Frey, M.J. Steiner, A. Shackelford, "Spectral nulling on transmit via nonlinear FM radar waveforms," *IEEE Trans. Aerospace & Electronic Systems*, vol. 47, no. 2, pp. 1507-1515, Apr. 2011.

[10] I.W. Selesnick and S.U. Pillai, "Chirp-like transmit waveforms with multiple frequency-notches," *IEEE Radar Conf.*, Kansas City, MO, May 2011.

[11] C. Nunn, L.R. Moyer, "Spectrally-compliant waveforms for wideband radar," *Aerospace & Electronic Systems Mag.,* vol. 27, no. 8, pp. 11-15, August 2012.

[12] L.K. Patton, B.D. Rigling. "Phase retrieval for radar waveform optimization," *IEEE Trans. Aerospace & Electronic Systems,* vol. 48, no. 4, pp. 3287-3302, October 2012.

[13] L.K. Patton, C.A. Bryant, B. Himed, "Radar-centric design of waveforms with disjoint spectral support," *IEEE Radar Conf.,* Atlanta, GA, May 2012.

[14] A. Aubry, A. De Maio, Y. Huang, M. Piezzo, A. Farina, "A new radar waveform design algorithm with improved feasibility for spectral coexistence," *IEEE Trans. Aerospace & Electronic Systems*, vol. 51, no. 2, pp. 1029-1038, Apr. 2015.

[15] A. Ephremides, J.E. Wieselthier, D.J. Baker, "A design concept for reliable mobile radio networks with frequency hopping signaling," *Proc. IEEE*, vol. 75, no. 1, pp. 56-73, Jan. 1987.

[16] R. Kohno, R. Meidan, L.B. Milstein, "Spread spectrum access methods for wireless communications," *IEEE Communications Magazine*, vol. 33, no. 1, pp. 58-67, Jan. 1995.

[17] T. Higgins, T. Webster, A.K. Shackelford, "Mitigating interference via spatial and spectral nulling," *Radar, Sonar & Navigation, IET* , vol.8, no.2, pp.84,93, Feb. 2014.

[18] J. Jakabosky, S.D. Blunt, B. Himed, "Spectral-shaped optimized FM noise radar for pulse agility," *IEEE Radar Conf.*, Philadelphia, PA, May 2016.

[19] S.W. Frost, B.D. Rigling. "Sidelobe predictions for spectrally-disjoint radar waveforms," *IEEE Radar Conf.,* Atlanta, GA, May 2012.